



Muon reconstruction in the Daya Bay water pools

R.W. Hackenburg

Brookhaven National Laboratory, Upton, NY, USA



ARTICLE INFO

Keywords:

Neutrinos
Water shield
Cosmic rays
Muons
Underground
Reconstruction

ABSTRACT

Muon reconstruction in the Daya Bay water pools would serve to verify the simulated muon fluxes and offer the possibility of studying cosmic muons in general. This reconstruction is, however, complicated by many optical obstacles and the small coverage of photomultiplier tubes (PMTs) as compared to other large water Cherenkov detectors. The PMTs' timing information is useful only in the case of direct, unreflected Cherenkov light. This requires PMTs to be added and removed as an hypothesized muon trajectory is iteratively improved, to account for the changing effects of obstacles and direction of light. Therefore, muon reconstruction in the Daya Bay water pools does not lend itself to a general fitting procedure employing smoothly varying functions with continuous derivatives. Here, an algorithm is described which overcomes these complications. It employs the method of Least Mean Squares to determine an hypothesized trajectory from the PMTs' charge-weighted positions. This initially hypothesized trajectory is then iteratively refined using the PMTs' timing information. Reconstructions with simulated data reproduce the simulated trajectory to within about 5° in direction and about 45 cm in position at the pool surface, with a bias that tends to pull tracks away from the vertical by about 3°.

© 2017 Elsevier B.V. All rights reserved.

1. Detector synopsis

The Daya Bay experiment [1,2] employs eight identically-designed antineutrino detectors (AD) to observe the antineutrino flux from six nearby nuclear reactors. The ADs reside in three separate experimental halls (EH) with two ADs in each of the two near halls and four in the one far hall (Fig. 1). The ADs are immersed in ultrapure water pools, which are instrumented with photomultiplier tubes (PMTs). The pools serve both as shields for the ADs against natural, low-energy radiation, and also as water Cherenkov detectors [3]. The pools are each divided into inner and outer water shields (IWS and OWS), separated by highly reflective Tyvek and very nearly optically isolated from each other. The OWS comprises the outer 1 m of each pool's sides and bottom, but does not cover the top. The IWS and OWS are each populated with 20 cm photomultiplier tubes (PMT), which detect the Cherenkov light produced by the passage of a relativistic charged particle through the water. Being underground, such a particle can safely be assumed to be a muon, where EH1, EH2, and EH3 have overburdens of 250, 265, and 860 mwe (meters water equivalent) [3]. The PMTs are a combination of new Hamamatsu PMTs and older EMI PMTs recycled from the MACRO experiment [4]. A rectangular array of resistive plate chambers (RPC) covers each pool, with a pair of small RPC panels about 2 m above the main RPC array forming the RPC Telescope.

Each AD, IWS, OWS, and RPC is an independent detector subsystem. There are a total of five subsystems each in EH1 and EH2 (AD1, AD2,

IWS, OWS, RPC), and seven in EH3 (AD1–AD4, IWS, OWS, RPC). ADCs and TDCs record the charge and time of each PMT that exceeds a threshold of about 0.25 pe (photoelectrons). The triggering and readout electronics of the PMT subsystems (ADs, IWS, and OWS) are all identical [5–7]. Each PMT subsystem is independently triggered by its own energy sum and multiplicity triggers, determined only by the subsystem's own PMTs and without regard to the other subsystems. Because of the processing time of the trigger logic, the trigger occurs $\sim 1 \mu\text{s}$ later than the recorded PMTs' times. The TDC values are recorded in such a fashion that they are negative, with the latest times the most negative. It is convenient to reverse this and shift the times positive, so that the earliest recorded times are a little above zero, with the latest times appearing as the most positive. To this end, the raw TDC values are subtracted from a fixed and somewhat arbitrary constant, which is the same for all events and PMTs, and for all detector subsystems. Thus, the reversed and shifted PMT time is

$$\tau \equiv (1100 - \text{TDC}) \times 1.5625 \text{ ns.} \quad (1)$$

Calculations involving the times are all differences, wherein the constant 1100 is always canceled. These ADCs and TDCs record multiple threshold crossings in a given readout from a trigger, but only the first such crossing, or hit, from each PMT is used here. The RPC subsystem is triggered when at least three of the four layers in an RPC module has a

E-mail address: hack@bnl.gov.

<http://dx.doi.org/10.1016/j.nima.2017.08.002>

Received 26 February 2017; Received in revised form 19 July 2017; Accepted 1 August 2017

Available online 12 August 2017

0168-9002/© 2017 Elsevier B.V. All rights reserved.

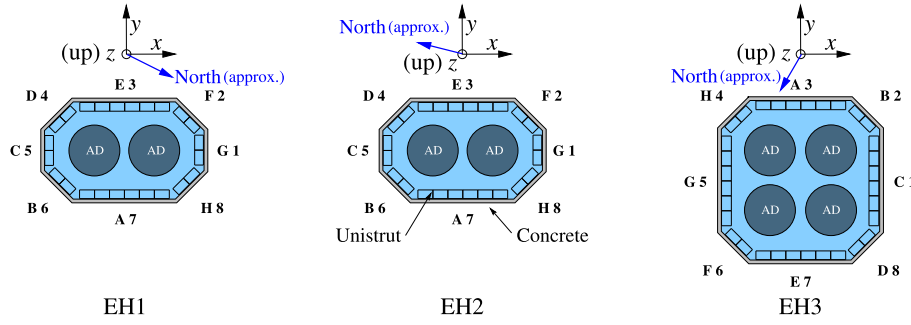


Fig. 1. Sketches (not to accurate scale) showing the water pools in the three experimental halls. The pools are all 16 m long in x and 10 m deep. EH3 is 16 m wide in y , while EH1 and EH2 are 10 m wide. The corner walls are at 45° to their neighboring walls. Each pool has eight walls, designated with letters A–H in engineering documentation, and with numbers 1–8 in software (which designates the floor as “wall 9”). Note that the correspondence between these two sets of labels is different in EH3 than in EH1 and EH2. The pools’ inner and outer optical zones are separated from each other by highly reflective Tyvek covering the Unistrut frame. The inner zones of EH1 and EH2 are each instrumented with 121 PMTs, while their outer zones each have 167, for a total of 288 in each hall. The inner zone of EH3 has 160 PMTs and its outer zone has 224, for a total of 384. The ADs are all 5 m in diameter, 5 m high, and 2.5 m above the bottom of the pool. An RPC array, not shown, covers each pool. In each hall, the origin is at the center of the designed pool surface (z is negative throughout the pool).

pulse. The separate subsystem readouts are combined into *events*. Not all events contain readouts from all detectors, and some consist of readouts from single detectors.

Each PMT is characterized by a gain μ and a timing offset t_0 , stored in a database and indexed by date and time. The gains are calibrated on a continuous basis using dark noise previous to each readout. The timing offsets correct for fixed differences in the timing of each PMT, caused by individual variations in PMT transit delay, signal propagation delay in the cable and electronics, etc., so that any two or more PMTs seeing a short pulse of direct light from an equidistant source would all have the same corrected time $\tau - t_0$, to within an error of about 2 ns. There is also a small correction made for the variation in timing due to pulse height, referred to as a *time walk* or *time slewing* correction, which is subtracted from the time to make small signals’ times earlier. For 2 pe, the smallest signals used in track reconstruction, this correction is 6.8 ns, but it falls rapidly to 0.6 ns at 20 pe and becomes negligible above 40 pe.

A set of calibration LEDs were installed in the pools to determine the PMT time offsets, among other uses, but these LEDs began to fail early in the course of the experiment, leaving ever-widening gaps in the set of PMTs which are illuminated by direct light from an LED. As will be demonstrated, these offsets can be obtained from an analysis of a large sample of muon data.

2. Initial trajectory

Absent any significant magnetic field, and considering only high energy cosmic muons, a muon trajectory is a straight line. In the local coordinate system of a hall (Fig. 1), a muon trajectory is specified separately in the xz and yz planes in terms of the common z coordinate and the four parameters $x_0, x' \equiv dx/dz, y_0, y' \equiv dy/dz$, thus

$$x(z) = x_0 + x'z \quad y(z) = y_0 + y'z. \quad (2)$$

The angles θ and ϕ (Fig. 2) are given by

$$\theta = \arctan \sqrt{x'^2 + y'^2} \quad \phi = \arctan y'/x'. \quad (3)$$

Without using the PMTs’ times, their positions and charges can be used to obtain an initial estimate of a trajectory through the method of Least Mean Squares (LMS). Let q_i be the charge from PMT i at the fixed position (x_i, y_i, z_i) , and let $w_i \equiv q_i^2$ be its weight.¹ Nine sums are

¹ This choice of weights is not mathematically rigorous, and there are other possible choices for the weights. However, this particular choice is a simple one, and found to work better than anything else that was tried, such as $w_i = q_i$ or $w_i = 1$ (unweighted). A general aspect of the methods described here is that, in places where a difficulty was encountered, plausible variations were introduced until there arose a method which overcame the difficulty and functioned as needed, with somewhat less regard for rigor and more regard for being able to demonstrate correct functionality.

accumulated over n PMT hits in a given event,

$$\begin{aligned} S_x &\equiv \sum_i w_i x_i & S_y &\equiv \sum_i w_i y_i & S_z &\equiv \sum_i w_i z_i \\ S_{x^2} &\equiv \sum_i w_i x_i^2 & S_{y^2} &\equiv \sum_i w_i y_i^2 & S_{z^2} &\equiv \sum_i w_i z_i^2 \\ S_{zx} &\equiv \sum_i w_i z_i x_i & S_{zy} &\equiv \sum_i w_i z_i y_i & S_w &\equiv \sum_i w_i. \end{aligned} \quad (4)$$

Only a small subset of all the PMTs is included in these sums. This subset is designated as the Use Set, described in detail below. The slopes and intercepts describing the trajectory are given by

$$\begin{aligned} x' &= (S_z S_x - S_w S_{zx}) / (S_z^2 - S_w S_{z^2}) \\ y' &= (S_z S_y - S_w S_{zy}) / (S_z^2 - S_w S_{z^2}) \\ x_0 &= (S_x - x' S_z) / S_w & y_0 &= (S_y - y' S_z) / S_w. \end{aligned} \quad (5)$$

Though not required by the method, an RPC hit may be incorporated in the sums in Eq. (4). The RPC hit is given a weight equal to the sum of the PMT weights. This constrains the trajectory to not deviate very much from the RPC hit, which represents the only truly known point on the trajectory. Although requiring an RPC hit reduces track-finding efficiency by 40%–50%, and introduces a bias through reduced angular acceptance, the trajectories of the surviving tracks are much improved.

3. PMT illumination geometry

The following development concerns a single PMT at position $\mathbf{r}_p = (x_p, y_p, z_p)$, where the subscripts are used here to distinguish between several useful points shown in Fig. 2, rather than between different PMTs as in Eq. (4). By definition, the muon crosses the surface at $\mathbf{r}_0 \equiv (x_0, y_0, 0)$. For a truly horizontal muon, the algorithm would need some small modifications, but since horizontal muons are handled in the limit, with \mathbf{r}_0 moving ever further away from the pool for increasingly-horizontal muons, there is no compelling need for such special treatment. Besides, if the RPC is used, there will be no tracks anywhere near horizontal. Considering that the expected resolution for d_{qp} (defined below) is about 50 cm, which corresponds to the 2 ns PMT timing resolution, the approximately 10 cm of air between $z = 0$ and the actual water surface is of no significant consequence, especially for muons which cross the surface outside the pool and enter the pool through the side. Likewise, the finite size (20 cm) of the PMT is not treated because that would introduce substantial complications without yielding significant benefits. The trajectory from Eq. (2) has a point of closest approach to a PMT $\mathbf{r}_c = (x_c, y_c, z_c)$ given by

$$\begin{aligned} z_c &= [(x_p - x_0)x' + (y_p - y_0)y' + z_p] \cos^2 \theta \\ x_c &= x_0 + x' z_c & y_c &= y_0 + y' z_c. \end{aligned} \quad (6)$$

Download English Version:

<https://daneshyari.com/en/article/5492723>

Download Persian Version:

<https://daneshyari.com/article/5492723>

[Daneshyari.com](https://daneshyari.com)